

STATE-OF-THE ART ON DETERMINISTIC FRACTALS IN FRACTURE

B.K. RAGHUPRASAD and G.S. BHATTACHARYA

*Civil Engineering Department,
Indian Institute of Science, Bangalore 560 012, India*

ABSTRACT

Mandelbrot, the pioneer in fractals, et al. showed that metal fracture surfaces are fractal in nature and introduced (1) the slit island method and (2) fracture profile analysis to estimate their fractal dimension. Lung gave two geometric forms of intergranular brittle fracture. Meisel presented perimeter - area and perimeter - yardstick analysis of rectifiable curves and of mathematically constructed simple fractal curves. Saouma et al. concluded after experiments that fracture profile in concrete is indeed fractal. Gol'dshtein et al. suggested that fracture consists of self-similar multilevel energy dissipation process and fracture is a multifractal process. Present authors have suggested an equation relating critical strain energy release rate and fracture surface energy in case of fractal crack for ductile or quasibrittle materials.

1. INTRODUCTION

Scientists and engineers who laid the foundation and built up the structure of 'Fracture Mechanics' always tacitly assumed that fracture profiles in materials are smooth plane in nature. Energy concept suggests that fracture should proceed through the path of least resistance. This 'path of least resistance' is not necessarily a smooth plane. Observational facts indicate that fracture profiles in metals and concrete are always very tortuous, rather than being plane.

Benoit Mandelbrot coined the term 'fractal' in 1975. A fractal set e.g., Koch curve or Peano monster curve is more 'irregular' than the sets considered in classical geometry. They often fit the shapes in physical world like coastline or Brownian motion better than regular arrangements of smooth curves and surfaces [1].

2. REVIEW OF PAPERS OF VARIOUS AUTHORS

Mandelbrot et al. [2] showed at first that metal fracture surfaces are fractal in nature and introduced (1) the slit island method and (2) fracture profile analysis to estimate their fractal dimension.

Slit Island Method

A fractured steel specimen was plated with electroless nickel and mounted in an epoxy mount by vacuum impregnation in order to ensure edge retention. The specimen was then polished parallel to the plane of fracture. 'Islands' of

steel surrounded by nickel appeared which on subsequent polishing, grew and merged. These structures are called slit islands. The islands contain 'lakes within islands' and 'islands within lakes'. The former was included and the latter was neglected.

When islands are derived from an initial fracture surface of dimension D by sectioning with a plane, their coastlines are of fractal dimension $D' = D - 1$. The graph of \log (perimeter) (x axis) versus \log (area) (y axis) of those islands was plotted. In a fractal this graph is rectilinear of slope D' . Authors concluded that such is indeed in the case of fracture surfaces.

Fracture Profile Analysis

This was based on Fourier analysis. Here the plated and processed fracture was sectioned perpendicular to the fracture surface to expose it in profile. The profile's sample spectra exhibited wide oscillations. Some were statistical artefacts, but others reflected fundamental lengths of the microstructure and their accompanying higher order harmonics. Average was taken over five spectra taken from serial sections, and they were integrated from high frequency to low. The fractal character of the surface was tested by plotting the data on doubly logarithmic coordinates to see if the curve has a large straight central portion of absolute slope B' , with $B' = B - 1 = 6 - 2D$. The plots were indeed straight but over narrower ranges than the area-perimeter plots. Thus the fracture surface was again

inferred to be fractal, and its fractal dimension was estimated by $D = 3 - (B'/2)$.

Lung et al. have been publishing papers on fractal nature of metal fracture since 1986 [3], [4], [5], [6] and [7]. In Ref.[3], author suggested that considering tortuosity of cracked surface would lead to the relation between critical crack extension force, G_c , and fracture surface energy, γ_s in the forms:

$$G_c = 2 (L(\epsilon)/L_o(\epsilon)) \gamma_s \quad \dots(1)$$

and

$$G_c = 2(W-a)^{-1} [L_1(\epsilon_1) + L_2(\epsilon_2)] \gamma_s + \gamma_p \quad \dots(2)$$

Equations (1) and (2) refer to brittle and ductile materials respectively. ϵ_i 's are the yardstick lengths in measuring tortuous crack length. Other parameters are as shown in Figures 1. In equation (1), L = tortuous crack length and L_o = straight crack length. γ_p represents the energy expended in the plastic work necessary to produce unstable crack propagation at the crack tip.

After this, Lung gave two geometric forms of intergranular brittle fracture as shown in figures 2 and derived the equation.

$$G_c = 2 \gamma_s \left(\frac{L_{oi}}{\epsilon_{oi}} \right)^{D-1} \quad \dots(3)$$

where L_{oi} = zero generation fractal length, ϵ_{oi} = each member's length in first generation and D = fractal dimension of fractal crack.

He preferred the profile shown in figure 2(a), because it consumes less energy than that in figure 2(b).

Later, he moved forward into ductile fracture. Here, he simply increased the angle shown in figure 2(a) by $\theta = (\rho bL/L) = \rho b$, where ρ is the linear density of mobile dislocations. The increment of angle by θ is the contribution of plastic displacement. Typical values of total linear density of dislocations range from 10^6 - 10^7 /cm for cold worked crystals to 10^3 /cm for annealed crystals. With $b \approx 3 \times 10^{-8}$ cm, the range of θ is from 3×10^{-5} radian to 0.03-0.3 radian (1.7° - 17°).

In ref.[4], the slit island method is employed to measure fractal dimensions D of fracture surfaces under plane strain conditions with the help of an image analysis technique for two high-strength steels under different heat treatment conditions and at different test temperatures. Three-point bend tests were performed on the specimens used for the fractal dimension investigation.

Then, the authors proceeded on the line of equation (1) and changed γ_s to γ_p which represents the effective surface energy (the sum of true surface energy and plastic strain energy on a unit crack area) needed to produce unstable crack propagation at the crack tip.

$$G_{IC} = 2(L(\epsilon)/L_o(\epsilon)) \gamma_p \quad \dots(1a)$$

According to Mandelbrot [1],

$$L(\epsilon_i) \approx \epsilon_i^{1-D} \quad \dots(4)$$

L_0 is chosen as a unit length. So,

$$G_{IC} = 2 \gamma_p \epsilon_i^{1-D} \quad \dots(5)$$

For plane strain fracture.

$$G_{IC} = \frac{K_{IC}^2}{E} (1 - \nu)^2 \quad \dots(6)$$

where K_{IC} = plane strain fracture toughness,

E = Young's modulus

and ν = Poisson's ratio of material.

Then,

$$\frac{K_{IC}^2}{E} (1 - \nu)^2 = 2 \gamma_p \epsilon_i^{1-D}$$

$$\begin{aligned} \text{or } 2 \ln K_{IC} + \ln (1 - \nu)^2 - \ln E \\ = \ln (2 \gamma_p) + (1 - D) \ln \epsilon_i \end{aligned} \quad \dots(7)$$

In this investigation E , ν and γ_p may be regarded as constant. Therefore,

$$\ln K_{IC} = \text{constant} + \frac{1}{2} (1 - D) \ln \epsilon_i \quad \dots(8)$$

The fracture toughness K_{IC} depends fundamentally on the fractal dimension D . Equation (8) is consistent with the experimental results. The fractal dimension D is approximately a linear function of the logarithm of fracture toughness K_{IC} .

Some authors [8], following Slit Island Method, pointed out that the correlation between fractal dimension, D_m , of

fractured surface and fracture toughness is a negative one. This, however, is difficult to explain. Lung and Mu [5] stated that D_m measured by SIM is not the intrinsic fractal dimension, D_0 , of the fractured surface of metals.

The measured dimension depends on the length of the yardstick and has a quantitative relation with D_0 . Starting from the basic equation relating perimeter and area of the Koch initiator island, they have shown that when yardstick length is small enough, D_m approaches D_0 . The origin of the negative correlation between D_m and toughness is due to the SIM of fractal dimension measurement. If the length of the yardstick is larger than a critical length, which is the yardstick coordinate of the point of intersection of two curves (straight lines) in D_m -yardstick plane, a negative correlation will be obtained. Thus, the critical lengths may be determined as the transition lengths between curves of negative and positive correlation.

In reference [6], the authors have again stated that the dimension measured with perimeter-area relation is not the real fractal dimension D_0 of the fractured surface and it is one of the origins of the negative correlation between D_m and the toughness of materials. For sufficiently small yardstick length, a positive correlation between D_m and toughness is observed.

Real fracture processes are quite complicated. A wide variety of mechanisms play relevant roles : grain boundaries,

inclusions, second phase particles, etc. The authors have analyzed the distance between two large inclusions and the number of grains over the distance. High yield strength materials have a smaller critical crack length for propagation. It may induce more smaller cracks to propagate. This makes the crack propagation between two small inclusions easier. In such case the correlation between fractal dimension of fracture surface and fracture toughness is indeed negative.

In reference [7], authors have found that the grain size and the average distance, between two large inclusions (LI) or between two effective second phase particles (ESPP), whose sizes are larger than that needed to form voids around them, have an effect on the fracture of metals in the fractal model. The roughness, shape and configuration of fracture curve depend on the external stress and also on the microstructure of the material. During fracture, a lot of voids are firstly created around the (ESPP or LI) as a metal deforms plastically, and then they increase in size and coalesce into void sheets, which ultimately form a fracture surface. Each plastic pit on the fractured microspheres corresponds to an ESPP or LI. The distance d_t between two pits determines the length of the fracture propagation zone. The sizes and orientation of the grains within d_t have an effect on the coalescence of the voids. The curves on the fractured surfaces are assumed to have the self-similarity property. Their fractal dimension is given by

$$D = \frac{\log N}{\log (1/r)} \quad \dots(9)$$

Where N is the (new) number of sides on the straight line segment when a figure is superimposed on it and r is the ratio of the figure edge length to the (preceeding) segment length.

The authors hypothesized that the r in equation (9) is proportional to the ratio of d_t to the grain size d, i.e. $r \propto d/d_t$. Two typical forms of intergranular fracture are shown in figure 3, which are exactly the same as figure 2.

Their fractal dimensions are

$$D (a) = \frac{\log (2m)}{\log (\sqrt{3} m)} \quad \dots(10)$$

$$D (b) = \frac{\log (2m)}{\log (3m/2)}, \quad m \text{ even}$$

$$D (b) = \frac{\log (2m+1)}{\log (3m/2 + 1/2)}, \quad m \text{ odd} \quad \dots(11)$$

Where $m = 1, 2, 3, \dots$ is the number of grains on the straight line segment d_t . The fractal dimension D is approximately a linear function of the logarithm of the grain number m.

The fractal dimension of the fractured surfaces can be expressed by the microstructural parameters d and d_t as

$$D = \frac{\log (C_1 d_t/d)}{\log (C_2 d_t/d)} \quad \dots(12)$$

where C_1 and C_2 are constants associated with the micro

structure, for example $C_1 = 1$, $C_2 = \sqrt{3}$ for figure 3 (a) and $C_1 = 4/\sqrt{3}$, $C_2 = \sqrt{3}$ for figure 3 (b).

Meisel [9] tried to formulate a generalized yardstick dependent perimeter area relation. The length of a fractal curve $P(E)$ measured with yardstick E is given by

$$P(E) = FE^{1-D} \quad \dots(13)$$

Where F and D are constant over the range of yardstick length E of interest. The length of a curve at yardstick E is the product of a measurable number $N(E)$ and E , i.e.,

$$P(E) = N(E) \cdot E \quad \dots(14a)$$

and so

$$N(E) = FE^{-D} \quad \dots(14b)$$

Similarly the area within a closed curve at yardstick E is the product of a measurable number and E^2 . A 'box counting algorithm' is applied in SIM. A rectangular grid of spacing E is superimposed over the island in question. The number of boxes containing a section of coastline is defined as $N(E)$. The area in units of E^2 of the island is defined as the number of boxes inside the coastline plus half the number of boxes on the coastline.

In fractal characterization of fracture surfaces, the ensemble of islands are taken as (statistically) self-similar. Each island can be classified according to its characteristic length L_0 . Self-similarity implies that for a given ratio of yardstick to characteristic length

$$\epsilon = \frac{E}{L_0} \quad \dots(15)$$

the ensemble of polygon approximations (corresponding to the ensemble of islands) based upon the appropriate yardsticks, (i.e., $E = \epsilon L_0$ for an island of characteristic length L_0) are (statistically) self-similar.

For self-similar island the number of divider steps

$$N(E, L_0) = N(\epsilon) = F' \epsilon^{-D} = F' E^{-D} L_0^D \quad \dots(16)$$

where the constant $F' (= F/L_0^D)$ is independent of E and L_0 . Similarly, the coastline length $P(E, L_0)$ of island having characteristic length L_0 is given by

$$P(E, L_0) = N(E, L_0) E = N(\epsilon) E = F' E^{1-D} L_0^D \quad \dots(17)$$

The area $A(E, L_0)$ of an island having characteristic length L_0 measured with yardstick E is taken as that of the equilateral polygon of side E constructed to evaluate $P(E, L_0)$.

For self-similar islands, polygon approximation of the same E are similar and the area of a polygon approximation of given ϵ is proportional to L_0^2 . Thus,

$$A(E, L_0) = G(\epsilon) \cdot L_0^D = G(\epsilon) E^2 / \epsilon^2 \quad \dots(18)$$

where $G(\epsilon)$ is the 'area shape factor'.

Equation (17) can be rewritten at fixed E as

$$\begin{aligned} P(E, L_0) &= F' E^{1-D} L_0^D = C(E) L_0^D \\ &= C(E) (E^2 / \epsilon^2)^{D/2} \end{aligned} \quad \dots(19)$$

where $C(E)$ is an E -dependent constant.

Thus, one may combine equations (18) and (19) to obtain

$$P(E, L_0) = C(E) [A(E, L_0) / G(\epsilon)]^{D/2} \quad \dots(20)$$

In conventional perimeter-area analysis, one takes twice the slope of the log-log plot of P vs A for fixed E as the fractal dimension. Following Lung and Mu [5], Meisel defines the 'measured fractal dimension' D_m by

$$\begin{aligned} D_m/2 &= [d \ln (P) / d \ln (A)]_E \\ &= [d \ln (P/E) / d \ln (A/E^2)]_E \quad \dots(21) \end{aligned}$$

Thus equation (20) implies that

$$\begin{aligned} D/2 &= -[d \ln (P) / d \ln (\epsilon^2)]_E \\ &= -[d \ln (P) / d \ln (G/\epsilon^2)]_E [d \ln (G/\epsilon^2) / d \ln (\epsilon^2)]_E \\ &= [d \ln (P) / d \ln (G/\epsilon^2)]_E [1 - d \ln (G) / d \ln (\epsilon^2)]_E \\ &= (D_m/2) [1 - d \ln (G) / d \ln (\epsilon^2)]_E \\ &= (D_m/2) [1 - d \ln (G) / d \ln (\epsilon^2)] \quad \dots(22) \end{aligned}$$

Victor Saouma et al. [10] proposed an experimental approach to properly understand fracture of concrete. They determined fractal dimension of a profile across a fracture surface using the box method of Barton and Larsen [11] by superimposing on the profile trace, a grid of square elements of various sizes. The number of grid elements crossed by the profile trace is counted (N), and plotted against the grid element size (r). Fractal dimension is calculated by the usual formula $D = \ln N / \ln (1/r)$.

The three specimens studied were cubes 36 in. on a side. Each of the specimens contained a different range of aggregate size. The maximum aggregate size in concrete type I was 0.75 in., in concrete type II it was 1.5 in and in concrete type III it was 3.0 in. The specimens were fractured by inflating a cylindrical packer in a four inch

diameter axial borehole, while the specimen was subjected to uniaxial compression perpendicular to the borehole axis.

The profilometer used for measurement of the roughness of fracture was fully automated. It scanned a sample by means of a motorized, computer-controlled placement of a Linear variable Differential Transformer.

Following the experimental test, the fractal dimension of the fracture surface roughness was determined using a computerized version of the box method [1,11]. The length and spacing between profiles, and the minimum size of the box sizes used in the fractal analysis are presented in Table 2 Saouma's paper. That is reproduced below as Table 1.

Table 1. Profiles' geometry and fractal dimensions

Characteristics	II crack direction			I crack direction			
	0.75 in	1.50 in	3.00 in	0.75 in	1.50 in	3.00 in	1.50 in
Profile length	8.0	8.0	8.0	8.0	24.0	24.0	1.0
Min. Box size	0.045	0.045	0.045	0.045	0.125	0.125	0.0055
Readings inch	240.0	120.0	120.0	348.0	40.0	40.0	240.0
Profile spacing	0.1	0.5	0.5	1.0	0.5	0.5	0.5
Fractal dimension (D)	1.33	1.10	1.11	1.12	1.09	1.07	1.18
	1.11	1.09	1.11	1.10	1.08	1.08	1.12
	1.12	1.09	1.11	1.18	1.07	1.08	1.15
	1.11	1.02	1.12	1.09	1.07	1.09	1.22
	1.10						
	1.10						
	1.10						
	1.12						
	1.12						
	1.10						
	1.10						

It was concluded that fracture surfaces in concrete were fractal over the range of scales measured. The fractal dimension for the specimens tested was approximately 1.20 at the microscopic scale and close to 1.10 at the macroscopic scale. The roughness of the fracture does not vary significantly with fracture propagation direction.

Gol'dshtein and Mosolov [12] pointed that a fractal crack is characterized by a multiple-scale hierarchical structure of the singularities of the elastic fields. The fracture process is accompanied by a cascade process of the transfer of elastic energy from large scales to smaller scales, finally, to the microscale, where the energy dissipates as it is expanded on the formation of a new fracture surface.

When the crack tip moves by Δl on the microscale l , the elastic energy released is

$$\Delta U = G_0 \Delta l \quad \dots(23)$$

They assumed the following asymptotic relations in the neighbourhood of the tip of the fractal crack. E denotes elastic modulus.

$$u_i \sim \frac{K}{E} r^{1-\alpha} \phi_i(\theta) \quad \dots(24)$$

$$\sigma_{ij} \sim K r^{-\alpha} f_{ij}(\theta)$$

where K is the fractal stress-intensity factor, and r is the distance from the crack tip. The specific density of the energy released in the case of a smooth-edged crack is

characterized by $G_0 \sim K_I^2/E$. Taking equation (24) into account, it is easily seen that

$$G_0 \sim \frac{K^2}{E} l^{1-2} \quad \dots(25)$$

Next, they calculated the elastic energy released, taking into account the crack on the n^{th} microscale $l_n = l/R^n$, where R is the scaling parameter that determines the change in the crack fragments during scaling. Subsequently, they got the following relation.

$$G_0 = G(1) \sim l^{D-1} \quad \dots(26)$$

Comparing equations (26) and (25), it is seen that

$$D - 1 = 1 - 2\alpha$$

where

$$\alpha = \frac{1}{2} (2-D)$$

On the basis of relations (24) and (27), they obtained an asymptotic formula for the openings, Δu , at the tip of a fractal crack:

$$u \sim r^{D/2}$$

It follows from (24) and (27) that the SIF is characterized by an (anomalous) dependence on the macro-dimension of the crack:

$$K_I^f \sim \sigma l^\alpha \quad \dots(28)$$

The criterion for the limit equilibrium of a fractal crack can be written as follows:

$$K_I^f = K_{IC}^f$$

where K_{IC}^f is the critical value of the SIF which characterizes the resistance of the material against the growth of a scale l crack.

As a result of relation (28), they obtained

$$K_{IC}^f \sim K_{IC} l^{(D-1)/2} \quad \dots(29)$$

where K_{IC} is the cracking resistance to macrofracture.

In contrast with K_{IC} , the fractal cracking resistance K_{IC}^f is a quantity of variable dimension, and since the fractal dimension D depends strongly on the fracture mechanism, K_{IC}^f is determined by the entire fracture process.

On going from one scale to another one can generally expect a change in the fracture mechanism, and, therefore a change in the dimension D . In other words, fracture should be considered as a multilevel (multifractal) process. The dimension of the fractured structure is scale-dependent :

$$D = D(l)$$

3. PRESENT AUTHORS' VIEW

Present authors feel that the characteristic inherent nonlinearity in fracture of quasibrittle and ductile materials can be expressed by writing the equation relating critical crack extension force (G_c) and fracture surface energy (γ_s) in the form

$$G_c = (2\gamma_s)^A \left(\frac{L_{oi}}{\epsilon_{oi}} \right)^{D-1} \quad \dots(30)$$

Here L_{oi} = zero generation fractal crack length, ϵ_{oi} = yardstick length in fractal crack, and D = fractal dimension [Ref. figures (1) and (2)].

Choosing L_{oi} as a unit length, equation (30) becomes :

$$G_c = (2\gamma_s)^A \epsilon_{oi}^{1-D} \quad \dots(31)$$

$$\begin{aligned} \text{Hence } \ln G_c &= A \ln (2\gamma_s) + (1 - D) \ln \epsilon_{oi} \\ &= A \ln (2\gamma_s) + B \quad \dots(32) \end{aligned}$$

$$\text{where } B = (1 - D) \ln \epsilon_{oi}$$

If $x = \ln (2\gamma_s)$ and $y = \ln G_c$, (32) gives

$$y = Ax + B \quad \dots(33)$$

The constants A and B will have to be determined by least square technique based on experimental data. An example from fracture of concrete will be presented here.

Calculations for usual least square fit of y lead to the following equations

$$A \sum_{i=1}^n x_i^2 + B \sum_{i=1}^n x_i = \sum_{i=1}^n x_i y_i \quad \dots(34)$$

$$A \sum_{i=1}^n x_i + n \cdot B = \sum_{i=1}^n y_i$$

In ref.[13], there is a chapter on 'Fracture Mechanics

Applied to Concrete' by R.Narayan Swamy. In tables (3) and (4), he gave one range in each case of G_c and γ_s for concrete. The present authors accepted them and in between each of them placed nine more values uniformly spaced.

Table 2. Calculations for constants A and B

Sl. No.	G_c (N/m)	$2\gamma_s$ (J/m^2)	$Y=\ln G_c$	$x=\ln(2\gamma_s)$	x^2	xy
1.	8.40	7.00	2.1282	1.9459	3.7866	4.1413
2.	8.52	7.55	2.1424	2.0215	4.0866	4.3309
3.	8.64	8.10	2.1565	2.0919	4.3759	4.5110
4.	8.76	8.65	2.1702	2.1575	4.6551	4.6822
5.	8.88	9.20	2.1838	2.2192	4.9249	4.8463
6.	9.00	9.75	2.1972	2.2773	5.1859	5.0037
7.	9.12	10.30	2.2105	2.3321	5.4389	5.1551
8.	9.24	10.85	2.2235	2.3842	5.6842	5.3013
9.	9.36	11.40	2.2364	2.4336	5.9225	5.4425
10.	9.48	11.95	2.2492	2.4807	6.1540	5.5796
11.	9.60	12.50	2.2618	2.5257	6.3793	5.7126
Σ			24.1596	24.8696	56.5939	54.7065

Now, one can put the numerical values obtained from Table 2 in equations (34) and solve them simultaneously for A and B.

Solving them, we get

$$A = 0.2309 \quad \text{and} \quad B = 1.6743$$

Hence equation (32) relating critical crack extension force and fracture surface energy can be written in the form :

$$\ln G_c = 0.2309 \ln (2\gamma_s) + 1.6743 \quad \dots(35)$$

Also one can write

$$B = (1-D) \ln \epsilon_{oi} = 1.6743$$

$$\text{or } \ln \epsilon_{oi}^{(1-D)} = 1.6743$$

$$\text{or } \epsilon_{oi}^{(1-D)} = 5.3350 \quad \dots(36)$$

From the expression $D = \frac{\ln(N)}{\ln(1/r)}$, one gets

$$D = \frac{\ln(N)}{\ln(1/\epsilon_{oi})} = - \frac{\ln N}{\ln \epsilon_{oi}}$$

$$\text{or } \ln N = -D \ln \epsilon_{oi} = \ln \epsilon_{oi}^{-D}$$

$$\text{or } N = \epsilon_{oi}^{-D} \quad \dots(37)$$

From equation (36)

$$\epsilon_{oi}^{-D} = \frac{5.3350}{\epsilon_{oi}} \quad \dots(38)$$

comparing equation (37) and (38)

$$\frac{5.3350}{\epsilon_{oi}} = N \quad \dots(39)$$

$$\text{So, for } N = 30, \quad \epsilon_{oi} = 0.1778$$

and

$$D = \frac{\ln 30}{-\ln(0.1778)} = 1.9695$$

In this way, the authors have calculated a set of values of fractal dimension D and length of each member in first generation of fractal crack against a set of values of N . They are shown in Table 3. The last column shows values of G_c (N/m) against $\gamma_s = 3.5 \text{ J/m}^2$. The fractal dimension D decreases with increasing segment number N . This tallies with the observations given in Table 1 of Ref.[7].

Table 3. Fractal dimensions for different fractal cracks

Sl. No.	Zero generation fractal length (L_{oi})	Number of members in first generation (N)	Length of each member in first generation (ϵ_{oi})	Fractal dimension (D)	G_c (N/m)
1.	1	30	0.1778	1.9695	8.3623
2.	1	35	0.1524	1.8901	8.3629
3.	1	40	0.1334	1.8311	8.3602
4.	1	45	0.1185	1.7852	8.3647
5.	1	50	0.1067	1.7482	8.3610

4. CONCLUSIONS

Fractal geometry is one of the most rapidly developing subjects in these days. Books, reports and papers covering various aspects of the theory and applications, including applications to fracture mechanics, are piling up in huge amount day by day. The authors do not claim that the paper presents state-of-the art on deterministic fractals in fracture complete in all details. But it is hoped that it will be helpful to the people interested in application of fractal geometry to fracture mechanics.

5. FIGURES

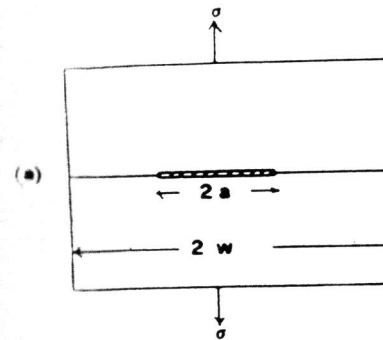


Figure 1a

Ideal brittle fracture in glass

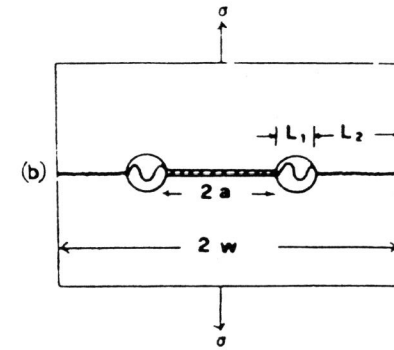


Figure 1b

Elastic-plastic fracture in metal

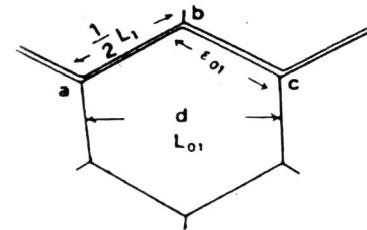


Figure 2a

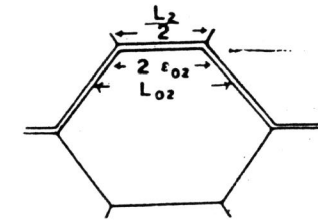
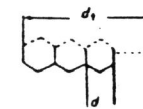
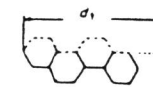


Figure 2b

Intergranular brittle fracture



(a)



(b)

Figure 3. Two typical forms of intergranular fracture

6. REFERENCES

1. Benoit Mandelbrot - The Fractal Geometry of Nature, Freeman, New York (1983).
2. Mandelbrot, Passoja and Paullay - Fractal character of fracture surfaces of metals, Nature, Vol.308, pp.721-722, 1984.
3. C.W. Lung - Fractals and the fracture of cracked metals, in Fractals in Physics, editors L. Pietronero, E. Tosatti, Elsevier Science Publishers, pp.189-192, 1986.
4. Mu and Lung - Studies on the fractal dimension and fracture toughness of steel, J. Phys. D : Appl. Phys. 21, pp.848-850, 1988.
5. Lung and Mu - Fractal dimension measured with perimeter-area relation and toughness of materials, Physical Review B, Vol.38, No.16, pp.11781-11784, 1988.
6. Lung and Zhang - Fractal dimension of the fractured surface of materials, Physica D, 38, pp.242-245, 1989.
7. Zhang and Lung - Fractal dimension and fracture toughness, J. Phys. D : Appl. Phys. 22, pp.790-793, 1989.
8. Pande, Richards, Louat, Dempsey and Schwoeble - Fractal characterization of fractured surfaces, Acta Metall., Vol.35, No.7, pp.1633-1637, 1987.
9. L.V. Meisel - Perimeter-area analysis, the slit island method and the fractal characterization of metallic fracture surfaces, J. Phys. D : Appl. Phys. 24, pp.942-952, 1991.

10. Saouma, Christopher, Barton and Gamaleldin - Fractal characterization of fracture surfaces in concrete, Engineering Fracture Mechanics, Vol.35, No.1/2/3, pp.47-53, 1990.
11. Barton and Larsen - Fractal Geometry of two-dimensional fracture networks at yucca mountain, Southwest Nevada, in Fundamental of Rock Joints: Proc. Int. Symp. Fundam. Rock Joints (Edited by Ove Stephannson, pp.77-84, Bjorkliden, Lapland, Sweden, 1985.
12. Gol'dshtein and Mosolov - Cracks with a fractal surface, soviet Physics Doklady, 36(8), pp.603-605, 1991.
13. F.D. Lydon (Editor) - Developments in Concrete Technology I, Applied Science Publishers Ltd., London, 1979.